frontiers | Frontiers in Marine Science

TYPE Original Research
PUBLISHED 25 November 2022
DOI 10.3389/fmars.2022.1015188

OPEN ACCESS

EDITED BY
Alessandro Bergamasco,
National Research Council (CNR), Italy

REVIEWED BY
Heather McNair,
University of Rhode Island,
United States
Oscar E. Romero,
University of Bremen, Germany

*CORRESPONDENCE
Silvan Urs Goldenberg
sgoldenberg@geomar.de

SPECIALTY SECTION
This article was submitted to Marine Biogeochemistry, a section of the journal Frontiers in Marine Science

RECEIVED 09 August 2022
ACCEPTED 19 October 2022
PUBLISHED 25 November 2022

CITATION
Goldenberg SU, Taucher J, Fernández-Méndez M, Ludwig A, Arístegui J, Baumann M, Ortiz J, Stuhr A and Riebesell U (2022) Nutrient composition (Si:N) as driver of plankton communities during artificial upwelling.
Front. Mar. Sci. 9:1015188.
doi: 10.3389/fmars.2022.1015188

Nutrient composition (Si:N) as driver of plankton communities during artificial upwelling

Silvan Urs Goldenberg[1]*, Jan Taucher[1], Mar Fernández-Méndez[1,2], Andrea Ludwig[1], Javier Arístegui[3], Moritz Baumann[1], Joaquin Ortiz[1], Annegret Stuhr[1] and Ulf Riebesell[1]

[1]Marine Biogeochemistry, Biological Oceanography, Geomar Helmholtz Centre for Ocean Research Kiel, Kiel, Germany, [2]Polar Biological Oceanography Section, Alfred Wegener Institute Helmholtz Centre for Polar and Marine Research, Bremerhaven, Germany, [3]Instituto de Oceanografía y Cambio Global, IOCAG, Universidad de Las Palmas de Gran Canaria, Las Palmas de Gran Canaria, Spain

Artificial upwelling brings nutrient-rich deep water to the sun-lit surface to boost fisheries or carbon sequestration. Deep water sources under consideration range widely in inorganic silicon (Si) relative to nitrogen (N). Yet, little is known about how such differences in nutrient composition may influence the effectiveness of the fertilization. Si is essential primarily for diatoms that may increase food web and export efficiency *via* their large size and ballasting mineral shells, respectively. With a month-long mesocosm study in the subtropical North Atlantic, we tested the biological response to artificial upwelling with varying Si:N ratios (0.07-1.33). Community biomass increased 10-fold across all mesocosms, indicating that basic bloom dynamics were upheld despite the wide range in nutrient composition. Key properties of these blooms, however, were influenced by Si. Photosynthetic capacity and nutrient-use efficiency doubled from Si-poor to Si-rich upwelling, leading to C:N ratios as high as 17, well beyond Redfield. Si-rich upwelling also resulted in 6-fold higher diatom abundance and mineralized Si and a corresponding shift from smaller towards larger phytoplankton. The pronounced change in both plankton quantity (biomass) and quality (C:N ratio, size and mineral ballast) for trophic transfer and export underlines the pivotal role of Si in shaping the response of oligotrophic regions to upwelled nutrients. Our findings indicate a benefit of active Si management during artificial upwelling with the potential to optimize fisheries production and CO_2 removal.

KEYWORDS

ocean fertilization, diatoms, stoichiometry, silicic acid, ecosystem-based aquaculture, negative emission technology, carbon dioxide removal

Introduction

Food security and climate change are recognized as two great challenges of the 21st century and beyond (Godfray et al., 2010; IPCC 2014). But how do we best develop food production and the capacity to neutralize green-house gas emissions to meet the global growth in human prosperity and population? Terrestrial and coastal resources are already utilized intensively by competing societal sectors, limiting the expansion of farmland and negative emission technologies (Minx et al., 2018; Fuhrman et al., 2020; Macreadie et al., 2021). Open-ocean ecosystems, in contrast, which cover over half of our planet, still hold vast amounts of untapped resources (Moore et al., 2013; Gattuso et al., 2021). They cannot be sourced, however, by the traditional 'hunter-gatherer' approach to ocean management. Here, seafood yield is limited by the existing productivity (Pauly and Christensen, 1995; Costello et al., 2020), while the ocean's natural ability to take up CO_2 is allowed to degrade unchecked (Matear and Hirst, 1999; Steinacher et al., 2010). Ground-breaking innovations in ocean food production and CO_2 removal are thus needed to achieve global environmental and social sustainability.

Ocean artificial upwelling is a nature-based solution with the potential to boost ecosystem services in regions of low biological activity. The warm, nutrient-poor surface waters in tropical and subtropical seas are characterized by low productivity (Steinacher et al., 2010; Armengol et al., 2019). Here, the nutrients are locked away in cold (i.e. heavier) deep water below the surface mixed layer (Moore et al., 2013; Dulaquais et al., 2014). Artificial upwelling, however, could break the density gradient and force nutrient-rich deep water to the sun-lit surface stimulating primary productivity (Pan et al., 2016). As in natural upwelling systems, the enhanced biomass production may be transfered to exploitable fish (Chavez and Messie, 2009; Messie et al., 2009) or exported to the ocean's interior where it may be stored longer-term (Boyd et al., 2019). The vertical mixing, in turn, could counter enhanced stratification under climate change and the expansion of 'ocean deserts' (Polovina et al., 2008; Boyce et al., 2010; Steinacher et al., 2010; Fu et al., 2016). Artificial upwelling may thus be evaluated as (1) ecosystem-based aquaculture that is, contrary to conventional fish farming, not limited by animal feed (Tacon and Metian, 2015), (2) a biological CO_2 sink more scalable than blue carbon in coastal areas (Macreadie et al., 2021), and (3) a nature conservation tool to restore pelagic habitats degraded by human-induced warming and stratification.

The 'classical' view of pelagic ecosystems identifies two food web models of contrasting potential for fisheries and carbon export (Ryther, 1969; Eppley and Peterson, 1979; Cushing, 1989). In oligotrophic, low productivity systems, small phytoplankton dominate and organic matter is recycled rather than exported. Here, multiple trophic steps, each entailing a loss of energy, are required to reach larger crustacean grazers. Eutrophic, high productivity systems are instead based on upwelled nutrients that favour large phytoplankton. These allow direct grazing by crustaceans that in-turn support small pelagic fish (Cury et al., 2000; Espinoza and Bertrand, 2008). Such short food webs are considerably more efficient in transferring energy (Eddy et al., 2020) leading to exceptional fisheries yields (Chavez and Messie, 2009). The biological pump is also highly active here. It removes CO_2 from the atmosphere where the exported organic carbon exceeds the upwelled inorganic carbon (Eppley and Peterson, 1979; Karl and Letelier, 2008); a balance that partly hinges on the carbon to nutrient ratio of biological processes (Hessen et al., 2004). Diatoms are given a key role in driving these ecosystem services. They dominate new production in natural upwelling systems and spring blooms in coastal seas and their large size makes them ideal food for crustacean plankton (Sommer et al., 2002).

Diatoms build silica (SiO_2) cell walls that characterize their role in elemental cycles and their nutrient requirements. To the organisms, the shells may serve multiple functions including grazer protection and nutrient and light harvesting (Mitchell et al., 2013; Romann et al., 2015; Pancic et al., 2019). Following cell growth, the mineral shells provide ballast to aggregates and fecal pellets, accelerating the sequestration of carbon through increased sinking velocities (Ragueneau et al., 2000; Armstrong et al., 2001; Jin et al., 2006). For the biomineralization of their shells, however, diatoms require dissolved silicate ($Si(OH)_4$), whilst other primary producers are often limited only by nitrate (NO_3) and phosphate (PO_4) (Moore et al., 2013). The relative availibility of silicate over other macro-nutrients therefore shapes the environmental and ecological niche of diatoms (Dugdale and Wilkerson, 1998; Sommer et al., 2002; Allen et al., 2005; Bibby and Moore, 2011). A nutrient ratio of silicate to nitrate of 1:1 has been considered optimal, yet with considerable variability between and within diatom species (Sarthou et al., 2005). In principle, lower silicate limits diatom growth and shifts the competitive balance towards other primary producers, while higher silicate reduces the energetic cost for biomineralization favouring diatom dominance.

Silicate shows a distinct distribution pattern across the world's oceans. At the sun-lit surface, silicate is often limiting (Griffiths et al., 2013; Dulaquais et al., 2014) and any newly introduced silicate is thus quickly depleted by diatoms (Dugdale and Wilkerson, 1998; Sarmiento et al., 2004; Allen et al., 2005). The vertical profile of silicate differs from that of the other macro-nutrients due to the slower remineralization of silica shells compared to organic nitrogen or phosphorus during the downward flux of particles (Ragueneau et al., 2000). Whilst silicate increases slower with depth than nitrate and phosphate at first (Si:N < 1), it catches up on the other macro-nutrients at greater depth and finally exceeds them (Si:N > 1) (Griffiths et al., 2013; Dulaquais et al., 2014). The latitudinal and longitudinal distribution of silicate is, instead, determined by the longer-term

biogeochemical history of the water bodies that are moved globally *via* ocean currents (Sarmiento et al., 2004; Bibby and Moore, 2011).

By sourcing deep water with specific Si concentrations during artificial upwelling, would it be possible to boost beneficial primary producers (i.e. diatoms) and thereby maximize the effectiveness of the fertilization? Natural systems often deviate from biogeochemical paradigms at smaller spatiotemporal scales. The grazing of diatoms by crustaceans for trophic transfer (Ban et al., 1997; Decima and Landry, 2020) and the carbon to nutrient ratio of organic matter for export (Geider and La Roche, 2002; Martiny et al., 2013) are particularly variable. Generalization of such central processes and properties severely limits our predictive understanding of how nature-based solutions may enhance fisheries production and carbon sequestration (Dutreuil et al., 2009; Yool et al., 2009; Chassot et al., 2010; Baumann et al., 2021). Artificial upwelling would force sudden eutrophication onto a plankton community which is adapted, in its species composition and physiology, to an oligotrophic environment. Such an artificial system may produce extremes, including harmful side-effects but also unexpected benefits, and thus requires a rigorous testing and re-evaluation of established principles.

Here, we investigate the effect of nutrient composition (Si relative to N) on oligotrophic plankton communities during artificial upwelling. In the subtropical North Atlantic (Canary Islands), we simulated recurring fertilization with nutrient-rich deep water of constant nitrate but varying silicate levels. Over the course of 33 days, we employed a pelagic mesocosm system that captures much of the natural biogeochemical and ecological complexity (Figure 1B). The developing plankton blooms were closely monitored for organic matter assimilation (quantity) and composition (quality), with a special focus on diatoms. Shifts in fundamental community properties indicated a benefit of active Si management during artificial upwelling with the potential to optimize trophic transfer to fisheries and export for CO_2 removal.

Methods

Study system

The experiment took place on the island of Gran Canaria located at the eastern side of the North Atlantic gyre, where it is continuously swept with oceanic water by the Canary Current (Barton et al., 1998) (Figure 1A). Phytoplankton biomass and fisheries production is low and stratification prominent in these warm, subtropical waters (Aristegui et al., 2001; Neuer et al., 2007; Popescu and Ortega Gras, 2015). Vertical profiles indicate only a slow increase of inorganic nutrients with depth, which would translate into higher costs for artificial upwelling compared to other regions (Llinás et al., 1999; Neuer et al., 2007). Our aim, however, is not to evaluate the feasibility of

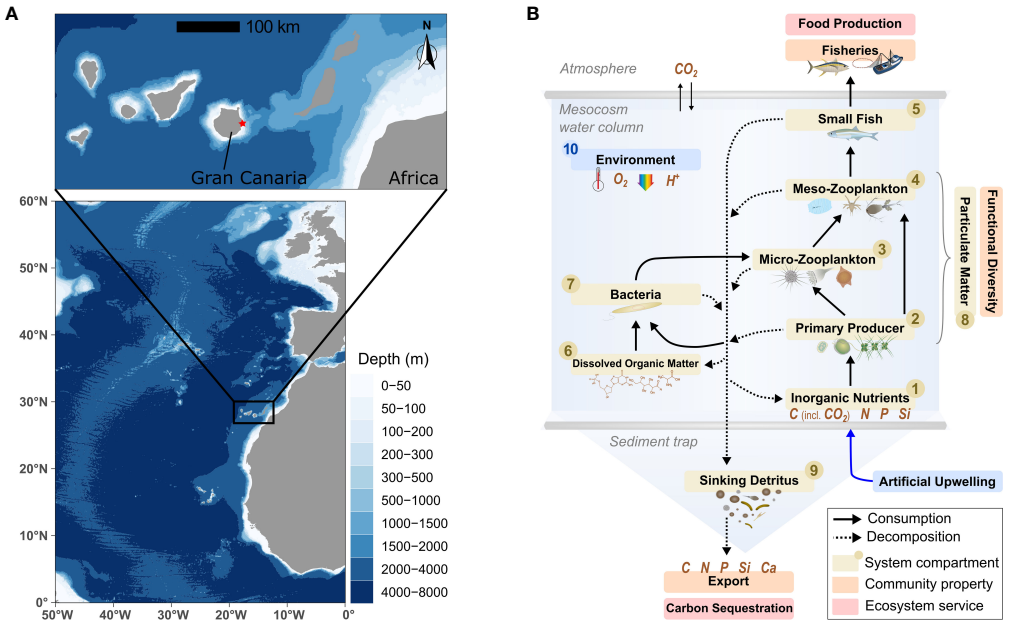

FIGURE 1
(A) Study site in the subtropical North Atlantic (red dot) (created with ggOceanMaps, Vihtakari, 2021). **(B)** Conceptualization of our pelagic mesocosms system. An overview of the parameters assessed for compartments #1-10 is provided by Table S1. Symbols from the Integration and Application Network (ian.umces.edu/media-library).

artificial upwelling locally but to conduct a general test of how an oligotrophic surface community responds to upwelling of nutrient-rich deep water.

Mesocosm facility

Eight floating mesocosms were installed in October 2019 inside Taliarte harbour (27°59'24" N, 15°22'8" W; Figures S1A, B), ~250 m from the laboratory facilities of the Plataforma Oceánica de Canarias (PLOCAN, https://www.plocan.eu) and the University of Las Palmas de Gran Canaria (ULPGC). Each mesocosm consisted of a transparent 1 mm polyurethane bag with cylindrical trunk and conical sediment trap, holding on average (± SD) 8292 ± 70 L of seawater. The bags were cleaned regularly to minimize growth of fouling organisms (Figure 2B). A large ring with rubber lips was scrubbed tightly along the inside walls (Riebesell et al., 2013) and the sediment traps and outside walls were brushed. This mesocosm system was previously deployed (Bach et al., 2019) and is the "in-shore" equivalent of the "Kiel Off-Shore Mesocosms for Oceanographic Studies" (KOSMOS) (Riebesell et al., 2013; Boxhammer et al., 2016; Taucher et al., 2017).

All mesocosm bags were filled in parallel with water from outside the harbour at 2-8 m depth (10-15 m bottom depth), using hoses (Ø 37 mm), a peristaltic pump (14 m^3 h^{-1}, KUNZ SPF60, Flexodamp FD-50) and mechanical flow meters. The natural plankton community was included, while larger organisms such as fish were excluded *via* a 3 mm mesh. The well-filled and firmly shaped mesocosm bags were measured by divers for a geometrical volume determination. Mesocosm volumes were then aligned by adjusting water removal during the first deep water addition on day 6.

Upwelling simulation

Small amounts of deep water were added to all mesocosms in short, regular intervals according to a continuous upwelling regime. Every second day, 320 L of mesocosm water was replaced by deep water, corresponding to a mixing ratio of deep water to mesocosm of 4%. Starting on day 6, this scheme totalled in 14 additions and a 56% replacement (Figure 2B). To assure a representative removal of mesocosm water and an even injection of the deep water, a special distribution device was moved up and down in the water column during pumping (Figure S1C).

To test the effect of nutrient composition, a gradient in silicon relative to nitrogen (Si:N) was established during the upwelling based on the eight mesocosms (Figure 2A). This Si:N treatment was achieved by adjusting the silicate ($Si(OH)_4$) concentration in the deep water specifically for each mesocosm while nitrate (NO_3), as well as phosphate (PO_4) and dissolved inorganic carbon (DIC), were kept constant.

Our Si:N range encompasses relevant natural and artificial upwelling scenarios (Sarmiento et al., 2004; Griffiths et al., 2013; Dulaquais et al., 2014). The lower boundary of 0.07 represented

A

Si:N treatment	0.07	0.33	0.50	0.67	0.83	1.00	1.17	1.33			
Nutrient	$Si(OH)_4$								NO_3	PO_4	DIC_{excess}
Deep water [µmol L^{-1}]	2	10	15	20	25	30	35	40	30	1.9	199
Mesocosm after addition [µmol L^{-1}]	0.08	0.38	0.58	0.77	0.96	1.15	1.35	1.54	1.15	0.07	7.65
Mesocosm accumulative [µmol L^{-1}]	1.1	5.4	8.1	10.8	13.5	16.2	18.8	21.5	16.2	1.01	91.8*
Si* = [Si] - [N] [µmol L^{-1}]	-28	-20	-15	-10	-5	0	5	10			
Mesocosm #	3	5	7	1	6	2	8	4			
Symbol											

DIC_{excess} ≙ dissolved inorganic carbon in excess of the hypothetical deep water baseline; *no extra DIC added in first two additions

B

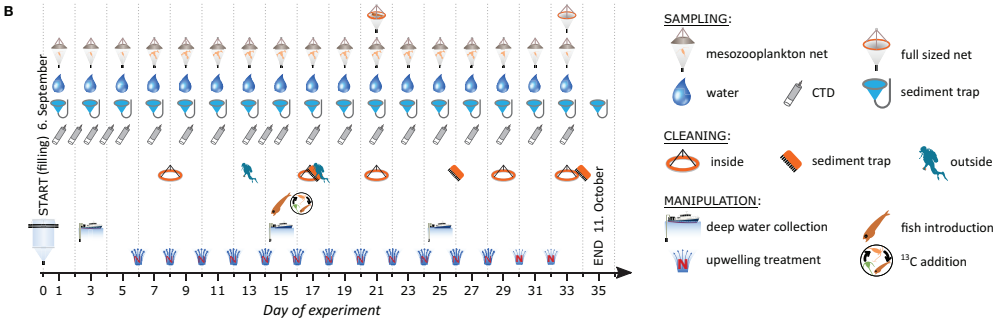

FIGURE 2
Experimental design to simulate artificial upwelling. **(A)** Nutrient regime with a gradient in silicate and constant levels of the other macro-nutrients (at Redfield). Each of the 14 additions exchanged 4% of the mesocosm (320 L). **(B)** Experimental schedule.

the lowest achievable Si:N given the silicate already present in the collected deep water. Increasing silicate is then hypothesized to benefit diatoms until a Si:N of 1 from which point onwards silicate may be less limiting (Sarthou et al., 2005). Specifically in the oligotrophic study system, Si:N in potential source water for artificial upwelling ranges from around 0.5 at 500 m depth to above 1.2 at depth greater than 2000 m (Llinás et al., 1999). Our upper Si:N boundary of 1.33 assures the inclusion of extreme scenarios.

Deviations from the planned addition scheme occurred. Due to initial uncertainty over the mesocosm volume, mesocosm 7 experienced a minimally higher mixing ratio of 4.2% during the 1st and 2nd addition. Further exceptions were the 10th addition, where 100 L less water was removed from each mesocosm to compensate for evaporation, and the 12th addition, where no water was removed before addition due to technical issues. Lastly, the 5th addition was based on surface water that had been treated with UV light and filtered at 5 µm, as the prior deep water collection failed. Despite these irregularities, the nutrient manipulation was overall fairly consistent, with standard deviations for mixing ratios between additions (n = 112) and mesocosms (n = 8) of 0.026% and of 0.010%, respectively.

Deep water

Deep water was collected on three occasions east of Gran Canaria at a minimum bottom-depth of 170 m (27°52'16" N, 15° 18'48" W or 28°00'01"N, 15°20'11"W). During each collection, a hose (Ø 37 mm) with a submersible pump (Grundfos SP-17-5R, flow rate 20 m^3 h^{-1}) was lowered to a depth of ~120-160 m and water was pumped into 12 opaque 1-m^3 food grade plastic containers. These were stored at 7°C degrees for use in the following days.

Our deep water source needed to meet the specific requirements of the study. On the one hand, a sufficient depth below the photic zone (~100 m) assured low chlorophyll *a* and low abundance of surface organisms (Neuer et al., 2007). On the other hand, we could not go too deep to keep nitrate levels well below our treatment target levels. The latter was necessary, given the silicate present besides nitrate in the collected water, to establish the wide Si:N treatment gradient *via* artificial supplementation of nutrients. The collected water contained (mean ± SD, n = 14 additions) 5.8 ± 1.6 µmol L^{-1} nitrate (NO_2 and NH_4 negligibly low concentrations), 0.38 ± 0.07 µmol L^{-1} phosphate, 2.12 ± 0.44 µmol L^{-1} silicate and 2358 ± 20 µmol L^{-1} DIC. Particulate organic nitrogen and carbon were at 0.24 ± 0.02 and 1.09 ± 0.12 µmol L^{-1} (mean ± SD, n = 3 collection containers), respectively, which is <1% of the final inorganic nutrient levels (Figure 2A) and ~10% of the particulate matter of the oligotrophic surface water in the mesocosms before the first upwelling treatment.

The collected deep water was amended to the desired nutrient levels immediately before each deep water addition (Figure 2A). Nitrate is the limiting nutrient in the study region (Figures 3F, G; Moore et al., 2013) and is also considered key in driving primary production in natural (Chavez and Messie, 2009) and artificial upwelling systems (Ortiz et al., 2022). Nitrate thus served as reference nutrient for our manipulation, representative of upwelling intensity. Deep water nitrate levels were topped up to 30 µmol L^{-1}, and phosphate and DIC were provided in Redfield ratio (C:N:P = 106:16:1) (Redfield, 1958). This nitrate concentration lies in the upper range of water supplied during natural upwelling (Messie et al., 2009) and could readily be sourced during artificial upwelling below a depth of a few hundred meters in some oligotrophic regions (Griffiths et al., 2013; Dulaquais et al., 2014). Nutrient salts were used to obtain the target nitrate ($NaNO_3$), phosphate (Na_2HPO_4) and DIC ($NaHCO_3$) concentrations. All salts were first dissolved in MilliQ water and equilibrated with HCl for proton-balance. Lastly, the Si:N treatment gradient was established by adding specific amounts of silicate salt (Na_2SiO_3) to the deep water designated for the respective mesocosms.

Trophic structure

A coastal pelagic zooplanktivore, the silverside *Atherina presbyter*, was caught locally and introduced to each mesocosm as early juvenile (n = 45, length = 17 mm) and young larva (n = 36, length = 9 mm) on day 15 after the sampling. Six days later, they were removed using a large net (1 mm mesh size) to assess growth and survival. Meso-zooplankton populations could not recover from the strong top-down control that had been exerted by the fish and remained at very low levels for the remainder of the experiment (day 21-33). Whilst the exact consequences for the smaller plankton, the focus of the current article, are unknown, we are certain about two aspects of this trophic restructuring. Firstly, it was identical for all mesocosms and thus not biasing the Si:N treatment. Secondly, it did not trigger the prominent temporal shift in the Si:N effect from the 'initial' to the 'longer-term' phase (Figures 4C–E). This effect originated from the carbon overconsumption during primary production that only afterwards accumulated in the particulate organic matter. As evident from chlorophyll *a* (Figure 4E) and O_2 production (Ortiz, unpublished data), the Si:N effect on carbon overconsumption peaks already on day 11 and has entirely vanished by the time the fish were introduced on day 15.

Sample collection

Sampling took place in the morning in two-day intervals (Figure 2B), always with the same order of parameters. Sampling

devices were gently lowered through the centre of the mesocosm to target depth using a smooth, abrasion resistant plastic line guided over an overhanging pulley (Figure S1B). Samples were transported to the nearby laboratory facilities in cooling boxes at ambient seawater temperature and immediately processed or preserved.

At dawn (~7-8:30 am), the sedimented material that had been collected over the past 48 h was transferred into 5 L glass bottles by means of a vacuum pump (Figure S1A, Boxhammer et al., 2016). Depth-integrated water samples were taken with a 2.5-m plastic tube (Ø 53 mm, 5.13 L) submersed vertically into the mesocosm (~8-10:30 am). Then, set-valves at both ends of the tube were shut – the lower valve *via* a string-system – and the extracted water column transferred to various parameter-specific storage containers. An average (± SD) of 8.7 ± 0.2 tubes corresponding to 44.4 ± 0.9 L were sampled per day and mesocosm. Meso-zooplankton was sampled *via* tubes and nets (Apstein Ø 17 cm, 56.7 L, 55 µm mesh size). To conclude the sampling day (~10-10:30 am), environmental conditions were recorded with three replicate CTD casts (CTD167M, Sea and Sun Technologies) to 3.5 m depth. The probe included sensors for depth, temperature, salinity, oxygen, pH, density, photosynthetically active radiation and chlorophyll *a* (see Schulz and Riebesell, 2013 for details).

Parameters

The major compartments of the pelagic system were assessed including mass and fluxes of both organic and inorganic matter (Figure 1B). This article focuses on suspended particulate matter and the community of larger phytoplankton. All other parameters measured in the context of this experiment are listed in Table S1.

To measure inorganic water chemistry, the water was directly subsampled into small bottles without air headspace. Particulate matter was removed *via* filtration (before day 17: 0.2 µm; on and after day 17: 0.45 µm, Sarstedt) and samples were stored at 4 °C until analysis on the same or the following day. The inorganic nutrients NO_3, NO_2, PO_4 and $Si(OH)_4$ were measured photometrically following Hansen and Koroleff (1999) and NH_4 fluorometrically following Holmes et al. (1999), each in triplicates. Total alkalinity (TA) was measured in duplicates *via* open cell titration (Metrohm 862 Compact Titrosampler with 907 Titrando unit) (Dickson et al., 2003). Dissolved inorganic carbon (DIC) was measured in triplicates *via* an Autonomous Infra-Red Inorganic Carbon Analyser (AIRICA; Marianda). TA and DIC measures were accurate within 1% of certified reference material (A. Dickson, Scripps Institution of Oceanography) (Dickson et al., 2007).

For the analysis of suspended particulate matter, the water was transferred into 10 L polyethylene containers and stored in a climate chamber at 15°C. Over the course of the day, these containers were subsampled for the different parameters. Sample volumes were continuously adjusted according to the development of the plankton bloom to avoid clogging, from 1 L at the start of the experiment to 0.2 L at the end. Samples were filtered with a negative pressure of 200 mbar onto glass fibre filters (>0.7 µm, GF/F Whatman, pre-combusted except for pigments) for total particulate carbon (TPC), particulate organic carbon and nitrogen (POC/N), particulate organic phosphorus (POP), and photosynthetically active pigments. Biogenic silica (BSi) was filtered in the same manner using cellulose acetate filters (>0.65 µm, Whatman). To remove particulate inorganic carbon (PIC), POC/N filters were acidified with 1 ml of 1 M HCl. Subsequently, POC/N and TPC filters were dried in an oven at 60 °C for 24 h. They were then packed in tin capsules and stored in desiccators until elemental analysis (Euro EA-CN HEKAtech) following Sharp (1974). Filters for POP and BSi were stored at -20 °C and analysed in the following days according to Hansen and Koroleff (1999). Filters for photosynthetic pigment analysis were stored at -80 °C until extraction and reverse-phase high-performance liquid chromatography (HPLC) (Ultimate 3000, Thermo Scientific) (Barlow et al., 1997). More details on the analytical procedures for these parameters are provided in Paul et al. (2015).

We found no consistent evidence for the presence of PIC. The difference between TPC and POC varied randomly around 0 and was unrelated to the Si:N treatment (Figure S2). We therefore considered PIC to be negligible and treated the TPC as second POC dataset. The precision of our POC (and also PON) estimate benefited considerably from the averaging across two separate filters and elemental analyses.

Larger phytoplankton was visually assessed using Utermöhl microscopy (Edler and Elbrächter, 2010; Bach et al., 2019). Water samples were filled in 250 ml brown glass bottles and fixed with acidic Lugol's iodine. A subsample of 20-50 ml was settled in a settling chamber for 24 h. Phytoplankton cells larger than ~5 µm were counted and identified to the lowest taxonomic level possible. The taxonomic composition of diatoms, the dominant group, was investigated, including indexes for species richness, evenness and diversity (Pielou, 1966). The dimensions of abundant taxa were measured regularly and those of rare taxa extracted from the literature for a geometrical estimation of cell biovolume following Olenina (2006). Finally, total biovolume of the diatom assemblage was calculated to serve as a proxy for biomass.

A potential shift in phytoplankton size distribution was assessed *via* flow cytometry. For this, 0.5-2 ml were analysed within 3 h of sampling using a Cytosense imaging flow cytometer (CytoBuoy, Woerden, Netherlands), with instrument settings optimal for the nano and micro scale. This technique structures natural plankton communities into clusters of similar cells based on fluorescence and light scatter properties (Dubelaar and Jonker, 2000; Veldhuis and Kraay, 2000). The three clusters representing the largest phytoplankton increased

most strongly following the nutrient addition and may thus be considered as the eutrophic specialists: 10-40 µm with high fluorescence, 10-40 µm with low fluorescence, and >40 µm chain-forming. For our analysis, the two 10-40 µm clusters were pooled to obtain two distinct groups of larger autotrophs, one ranging from large nano- to small microphytoplankton (10-40 µm) and one comprising larger microphytoplankton (>40 µm). These clusters represented the natural size structure in our system, which is not congruent with the commonly applied plankton size structure. Finally, cell abundances were standardized against the chlorophyll *a* of the entire autotroph community as measured by HPLC. These variables hence express the relative contribution of larger phytoplankton to the overall photosynthetic capacity.

Data analysis

All parameters followed the same basic data structure: a gradient of Si:N with 8 independent mesocosms that was repeatedly sampled over the course of the experiment. We used linear mixed models with random intercept to establish the general effect of Si:N and its change over time (restricted maximum likelihood fit, type III test, Kenward-Roger approximation, Bates et al., 2015; Kuznetsova et al., 2017; Singmann and Kellen, 2019). Si:N was employed as continuous explanatory variable, Mesocosm as random effect, and experimental Day and its interaction with Si:N as factors of the repeated design (Quinn and Keough, 2002). Potential deviations from normality of residuals and random effects were checked with normal Q-Q plots and homogeneity of variance with residual versus fitted plots. Data was transformed if necessary. Finally, we investigated the day-to-day development of the Si:N effect size. For this, individual linear regressions were conducted for each sampling day and their slopes plotted with 95% confidence intervals. All data analyses were performed at a significance level of $\alpha = 0.05$ with R version 4.0.5 (R Core Team, 2021; RStudio Team, 2021).

Results

A pronounced plankton bloom developed in all mesocosms following the addition of nutrient-rich deep water. The universally essential nutrients N and P dominated the overall build-up of biomass (particulate organic N, P and C) and the potential for primary production (chlorophyll *a*). In contrast, Si that is required specifically by diatoms determined the composition of the plankton community (C:N ratio, biogenic silica, diatoms, size). Consequently, Si in deep water may be seen as primary driver of plankton bloom quality that acts on top

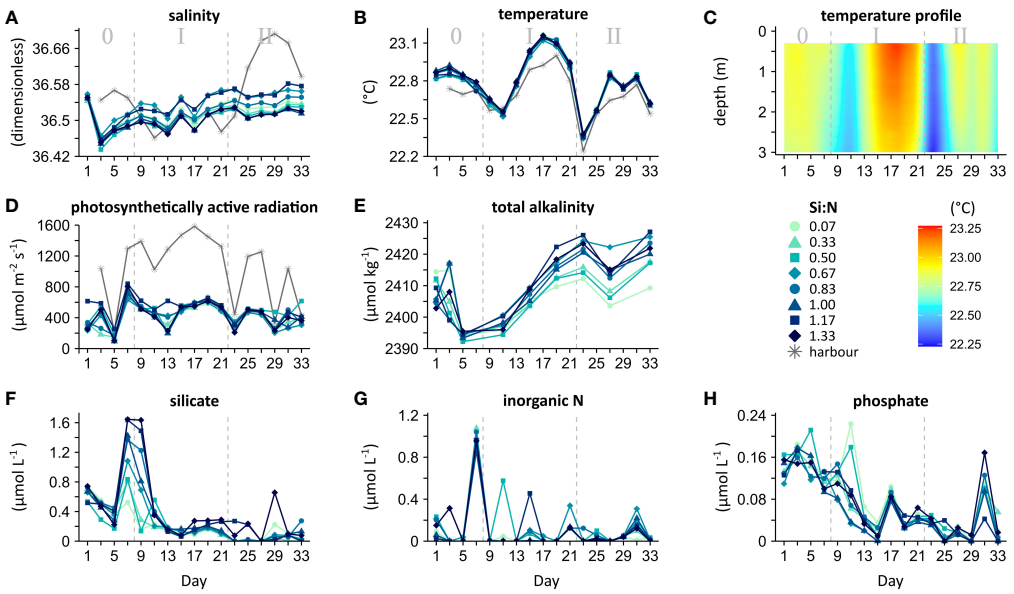

FIGURE 3
Environmental conditions and nutrient concentrations in the mesocosms. *In situ* measurements with averages from 0.3 to 2.5 m depth for each mesocosm **(A, B, D)** and a vertical profile averaged across all mesocosms **(C)**. Laboratory measurements of integrated water samples from 0 to 2.3 m depth **(E-H)**. Experimental phases: 0 = oligotrophic baseline, I = initial response, II = longer-term response.

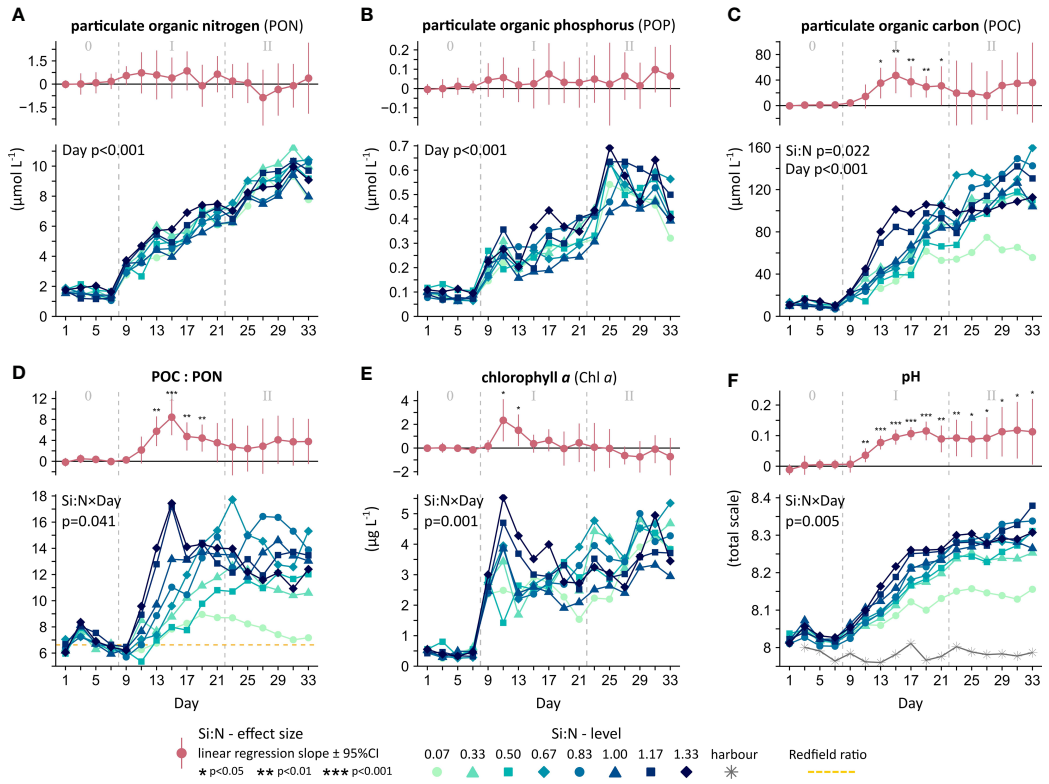

FIGURE 4
Biomass development under upwelling with varying deep water Si:N, including **(A-D)** particulate organic matter, **(E)** photosynthetic capacity, and **(F)** metabolic balance. Provided are the overall significances across time (Si:N, Day or Si:N×Day) and the daily Si:N effect (in red). Experimental phases: 0 = oligotrophic baseline, I = initial response, II = longer-term response.

of N and P upwelling determining quantity. To facilitate interpretation of the Si:N-effect, we distinguish between the three phases 'oligotrophic baseline' (0), 'initial response' (I) and 'longer-term response' (II), based on the distinct temporal pattern.

Environmental conditions

Environmental conditions were similar for all mesocosms and stayed relatively constant over the entire experimental period (Figures 3A–E and Tables S2A-D). Yet, there were slight variations from day to day, as characteristic of mesocosm systems. Salinity increased slowly over time due to evaporation (Figure 3A). Fluctuations in temperature closely followed the surrounding harbour water (Figure 3B). The absence of thermal stratification was indicative of a homogenous water column (Figure 3C). Photosynthetically active radiation varied with cloud cover as suggested by the matching harbour light pattern (Figure 3D). The phytoplankton bloom, in contrast, did not markedly reduce light availability. Whilst total alkalinity diverged following the Si:N gradient (Table S2D), absolute differences were small and likely biologically insignificant (Figure 3E).

Inorganic nutrients

The macro-nutrients added through the upwelling simulation were fully consumed by the plankton community (Figures 3F–H). Upon the first deep water addition (day 6), N (nitrate, nitrite and ammonia) and Si (silicate) peaked steeply. Whilst this increase was equal across mesocosms for N, Si varied matching the Si:N gradient (Figure 2A), which confirms a correct treatment application. During the following upwelling events every other day, the added nutrients were taken up quickly. In this eutrophic state (phase I and II), Si and P (phosphate) dropped to well below their oligotrophic levels (phase 0). It appears that our communities became first N, then N-Si and finally N-P-Si limited. We found no evidence for an effect of deep water Si:N on the consumption of N and P (Tables S2F, G). Si depletion was slightly slower in the high Si:N mesocosms (Table S2E), which however did not lead to Si accumulation (Figure 3F). Overall, our results suggest that,

after a brief period of adjustment, nutrient provisioning through recurring upwelling and primary productivity were in-phase, with efficient uptake of all macro-nutrients independent of their stoichiometry.

Biomass

Particulate organic matter – that is, the bulk measure across all suspended organisms and their remains including bacteria, phytoplankton, micro-zooplankton and smaller meso-zooplankton – grew steadily over the 27-days of upwelling (Figures 4A–C). Particulate organic nitrogen (PON) and phosphorus (POP) concluded with a ~5-fold higher mass compared to the oligotrophic baseline (Figures 4A, B - bottom). This accumulation of PON and POP was driven by the upwelling of N and P that was applied uniformly to all mesocosms and is incorporated in the factor 'Day' (Tables S3A, B). The Si:N treatment instead had no influence on PON and POP, neither overall (Table S3A, B) nor on a day by day basis as demonstrated by the insignificant daily regression slopes (Figures 4A, B - top). Consequently, their elemental ratio (PON : POP) also remained unchanged (Figure S3 and Table S3C). In agreement with the inorganic nutrients, these clear-cut results suggest that N and P cycling occurred independently of the Si levels in the deep water.

The production of carbon biomass, in contrast, was considerably accelerated under Si-rich upwelling. Over the first 2 weeks, the community with the largest excess in Si (Si:N = 1.33) grew 3-fold more particulate organic carbon (POC) than the one with the most severe Si deficiency (Si:N = 0.07) (Figure 4C - phase I, Table S3D). In parallel, carbon to nitrogen ratios of communities under high Si upwelling rose to more than twice that of the ocean-wide average Redfield stoichiometry (C:N ratio from ~6.6 to 17) (Figure 4D - phase I). This exceptionally rapid growth in POC has thus been achieved through a more efficient use of the upwelled N and P. The clear linear effect of Si:N on POC and organic matter stoichiometry was lost, however, over the longer term (Figures 4C, D - phase II). Instead, a curvilinear relationship characterized the second phase of our simulation with highest C:N ratios at intermediate levels of Si:N (Figure S4). Communities across the Si:N gradient finalised with about 10-fold higher POC and a doubling in C:N ratios compared to the oligotrophic baseline. Only the extreme low Si:N community followed an altogether different path in agreement with Redfield, possibly indicating a lower threshold in Si availability below which community functioning shifts drastically.

The development of chlorophyll *a*, as proxy for phytoplankton biomass and potential of photosynthesis, was influenced by the Si:N treatment in a pattern similar to POC (Figure 4E and Table S3F). We observed a sharp rise in chlorophyll *a* over the first 4 days of upwelling, peaking at double the concentration under excess Si compared to extreme Si deficiency (phase I). While there was still ample Si remaining from the oligotrophic state (day 7-9) (Figure 3F), the rate of chlorophyll *a* build-up was equally rapid in all mesocosms. Si only became truly limiting for a further rapid growth of chlorophyll *a* once this left-over had been depleted in the low Si:N mesocosms (day 9-11). This strong positive effect of Si:N on chlorophyll *a* was only characteristic of the immediate response to the regime shift. In the longer term (phase II), mesocosms evened out at around 4 μg L^{-1} chlorophyll *a* irrespective of the Si:N treatment.

Throughout the month-long upwelling simulation, communities across the wide range of Si:N maintained net-autotrophy. This positive metabolic balance, where primary production exceeds respiration, is indicated by the steady increase in pH (Figure 4F). Silicate-rich upwelling further accelerated the rise in pH over the first two weeks (phase I), indicating particularly high photosynthetic activity and associated consumption of CO_2 (Table S3G). Net-autotrophy and the accumulation of PON, POP and POC indicate a surplus in energy and organic matter that could be transferred from the plankton to fish (trophic transfer) and the deep ocean (carbon sequestration).

Larger phytoplankton

Diatoms responded strongly to the added nutrients. Throughout the entire manipulation, the biomineralization of dissolved Si (silicate) into particulate Si (biogenic silica) increased linearly with the Si:N treatment (Figure 5A and Table S4A). Being the major producers of biogenic silica, the microscopically assessed diatoms matched this pattern. Whilst diatoms were practically absent in the oligotrophic state, they quickly grew large populations in the mesocosms under high but not low Si-upwelling (Figure 5B and S3B; Table S4 B, C). Here, effect sizes were particularly large with a 6- and 7-fold increase in biogenic silica and diatoms, respectively, along our Si:N gradient. Other larger autotrophic taxa, in contrast, showed no consistent response to Si:N and were generally outnumbered by diatoms, even under Si-deficiency (Figure S3C and Table S4D).

Diatom composition was also shaped by the upwelling simulation. Assemblages under high Si upwelling were slightly richer in species (Figure S3D and Table S4E, 38 diatom taxa recorded) and more evenly composed (Figure S3E and Table S4F), resulting in higher diatom diversity (Figure S3F and Table S4G). However, only two genera dominated the upwelling-induced blooms across Si:N (Figure 5C). *Pseudo-nitzschia* was most prominent initially and *Leptocylindrus* over the longer-

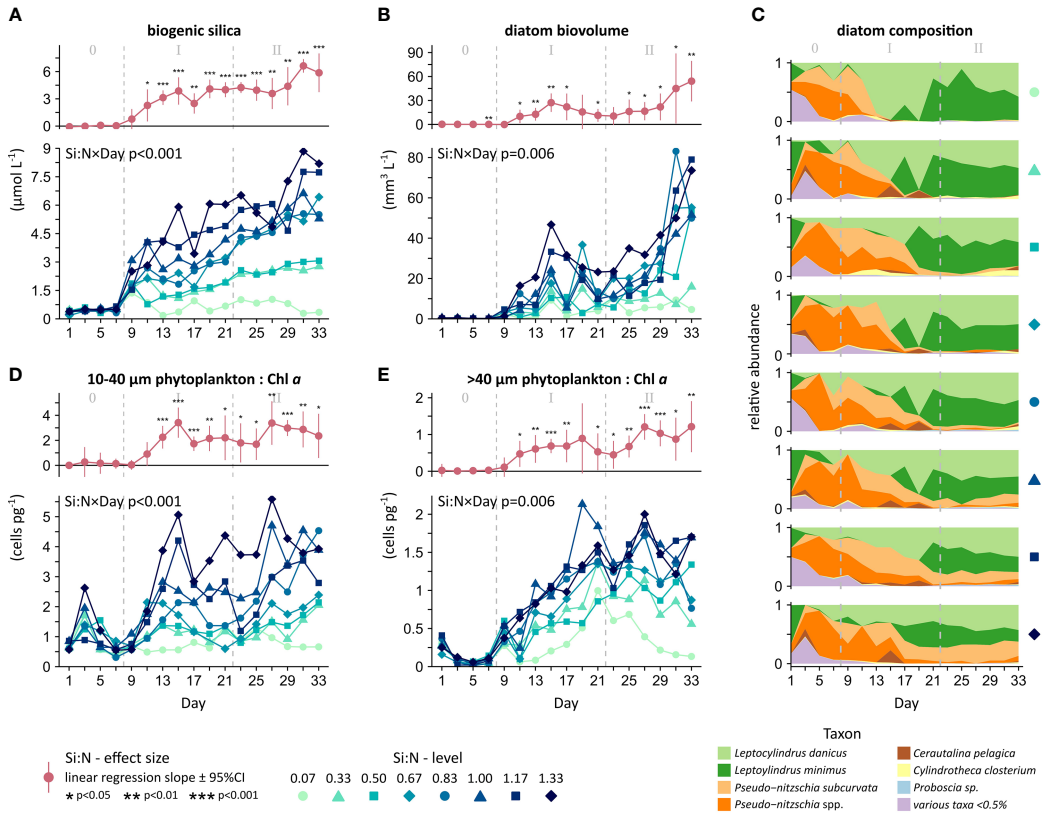

FIGURE 5
Larger phytoplankton under upwelling with varying deep water Si:N, including **(A)** biomineralized Si, **(B, C)** diatoms only (via microscopy), and **(D, E)** the abundance of all larger phytoplankton (via flow cytometry) relative to the chlorophyll *a* of the entire autotrophic community. Provided are the overall significances across time (Si:N, Day or Si:N×Day) and the daily Si:N effect (in red). Experimental phases: 0 = oligotrophic baseline, I = initial response, II = longer-term response.

term. Still, *Pseudo-nitzschia* was able to maintain significant populations under Si:N ratios of ≥1. Concluding, the observed increase in diatoms due to Si was primarily driven by an increase in the same species.

Phytoplankton size was strongly and positively affected by the Si in the deep water. As expected, phytoplankton at the nano and micro scale were only a minor component of the phytoplankton community during the oligotrophic state (Figures 5D, E). Upon the start of upwelling, populations of these larger phytoplankton grew most rapidly when provided with an excess of Si. Their contribution to overall photosynthetic capacity increased on average 6-fold (cluster 10-40 µm) and 3-fold (cluster >40 µm) from low to high Si:N (Figures 5D, E and Tables S4H, I). The general agreement with biogenic silica and diatom microscopy suggests that diatoms were responsible for differences in phytoplankton size. This Si-driven dominance of diatoms and their key traits (large size and mineral shells) persisted over time, in contrast to the response in carbon biomass (compare Figures S4, S5). Accordingly, Si availability was identified as a stronger driver than N and P for responses related to community composition (variation explained by 'Si:N', Tables S3E, S4).

Discussion

Our study demonstrates how the nutrient composition in deep water can drive plankton bloom dynamics during artificial upwelling. We now evaluate these responses to varying Si:N and explore possible implications for fisheries production and carbon sequestration (Figure 6).

Organic matter production

Basic plankton bloom functionality was upheld across our wide range in Si-availability. The cycling of N and P within the community was not measurably altered under extreme Si deficiency, which is surprising given the key role of diatoms in eutrophic systems (Dugdale and Wilkerson, 1998; Sarthou et al.,

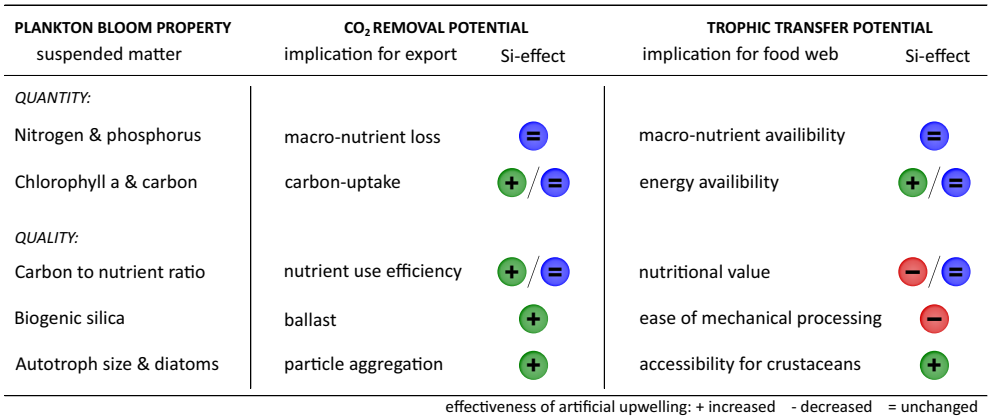

FIGURE 6
Possible consequences of varying Si:N in deep water for the effectiveness of artificial upwelling. Our findings for suspended matter are conceptually related to trophic transfer towards fisheries and carbon removal *via* the biological pump. Signs indicate increased (+), decreased (–) or unchanged (=) effectiveness. Two signs are given in case of a temporal pattern in the Si-effect: left for initial (first 2 weeks) and right for longer-term (following 2 weeks). This overview is limited to the simplified, 'classical' model of pelagic systems.

2005; Bibby and Moore, 2011). Even the influence of Si on photosynthetic capacity and carbon biomass dissipated with time. N and P availability, instead, was the primary driver of biomass synthesis, as presumed in previous studies on natural (Pitcher et al., 1991; Messie et al., 2009) and artificial upwelling (Karl and Letelier, 2008; Yool et al., 2009; Ortiz et al., 2022). Consequently, all our Si:N levels could maintain a photosynthetic capacity (2.5-5 μg L^{-1} chlorophyll *a*) similar to that of shelf seas and natural upwelling regions that support high zooplankton and fish production (Chavez and Messie, 2009; Gohin, 2011). Solely based on the energy and matter available for trophic transfer and export, the relative amount of Si in source water may not be critical for artificial upwelling facilities that maintain the bloom state long-term.

CO_2 removal potential

Our communities developed high carbon to nutrient ratios under upwelling in general, indicating a potential for carbon drawdown from the atmosphere. Nutrient-use efficiencies of our artificial systems were about twice that of the ocean wide average Redfield stoichiometry (Redfield, 1958) that would have to be exceeded for net carbon removal (Hessen et al., 2004; Karl and Letelier, 2008). Natural upwelling areas, in contrast, stay close to Redfield and may even act as a net source of CO_2 (Takahashi et al., 1997; Martiny et al., 2013). Accordingly, theoretical models on artificial upwelling employ Redfield stoichiometries and grant this technology only very limited potential for CO_2 sequestration (Dutreuil et al., 2009; Yool et al., 2009). Phytoplankton is exceptionally plastic, however, and can produce an excess in carbon-rich molecules under nutrient limitation (Geider and La Roche, 2002; Talmy et al., 2014; Mari et al., 2017). Such carbon overconsumption was possibly encouraged in our simulation, where the regularly added nutrients were rapidly exhausted by the elevated phytoplankton biomass causing intermittent N-limitation.

Si in deep water was an additional driver of carbon to nutrient ratios in our plankton blooms. During the first days of upwelling, the hypothetical carbon capture potential increased ~6-fold from communities with low (C:N = ~8) to high Si (C:N = ~16), when accounting for the inorganic carbon brought to the surface (C:N = 6.6, Redfield). Large phytoplankton such as diatoms are particularly well suited for the build-up of carbon-rich energy stores (Granum et al., 2002; Talmy et al., 2014) or the release of carbohydrates that aggregate to transparent exopolymer particles (TEP) (Mari et al., 2017). This possibly explains the strong Si-effect in the early phase of our bloom and the observed increase in C:N ratios in temperate mesocosms studies under nutrient limitation (Gilpin et al., 2004; Makareviciute-Fichtner et al., 2021). Clearly, fertilization strategies and seed communities that enable the biological pump to operate beyond the canonical Redfield ratio need better characterization. Only then, theoretical models may re-evaluate the potential of artificial upwelling as a negative emission technology.

The temporal shift in the influence of Si may reflect the progress in ecological adjustment. The environmental stability of the oligotrophic open ocean allows for a relatively precise adaptation of communities to low levels of regenerated nutrients (Landry, 2002;

Mojica et al., 2015). A strong upwelling of new nutrients stresses this balance and demands a drastic re-organisation towards traits beneficial under the alternate trophic state (Smetacek, 1999; Smith et al., 2009). Our results suggest that boosting diatoms *via* Si accelerates this transition so that high photosynthetic capacity, biomass and carbon to nutrient ratios are reached faster. Approaching the new steady-state, in contrast, our communities compensated for the varying nutrient stoichiometry, likely through functional redundancy (Rosenfeld, 2002). Low Si availability may have been offset either within diatoms, *via* lighter per capita silica shells (Sarthou et al., 2005) or higher per capita assimilation activity (Sathyendranath et al., 2009), or by non-silicifying primary producers (Dutkiewicz et al., 2021). The larger 'seed' communities involved in a real-world application would further increase the probability of including organisms that are essential to maintain ecological functioning across fertilizations scenarios.

Favourable properties for the formation and ballasting of sinking particles under high Si upwelling were maintained throughout the entire experiment. Suspended biogenic silica, and thus its availability for export, scaled proportionally with the Si treatment. Such mineral ballast in cells or zooplankton fecal pellets can considerably increase particle sinking velocity and therefore shorten the time-window for respiration of organic carbon before sequestration depths are reached (Armstrong et al., 2001; Jin et al., 2006). Diatoms are also thought to be efficient exporters due to their larger size, appendices and transparent exopolymer particles that facilitate aggregation and can further enhance sinking velocities (Thornton, 2002, but see also Mari et al., 2017 and Baumann et al., 2021). In conclusion, high Si upwelling altered the quality of suspended matter with a potential benefit for carbon removal, including carbon to nutrient ratios, the availability of mineral ballast and phytoplankton size. Our findings are, however, limited to the production of matter in the surface water, the first step towards carbon sequestration. Whether the subsequent export is efficient is uncertain and depends on complex ecological and biogeochemical processes involved in the formation and sinking of particles.

Trophic transfer potential

A pronounced shift towards larger phytoplankton occurred under high-Si upwelling, as hypothesized by benefiting diatoms. Cell size continued to increase even under Si:N ratios in excess of average diatom requirements (Si:N = 1:1, Sarthou et al., 2005). The shift in food size from the pico towards the nano and micro scale should make the primary production directly accessible for calanoid copepods (Kleppel, 1993; Harris et al., 2000; Sommer et al., 2002) and krill (Stuart, 1989; Riquelme-Bugueno et al., 2020). These crustacean taxa dominate grazing, including on diatoms, in productive shelf and upwelling systems, and provide a trophic shortcut to small pelagic fish (Cury et al., 2000; Espinoza and Bertrand, 2008). Under this traditional view of pelagic food webs (Cushing, 1989; Sommer et al., 2002), artificial upwelling with high Si may thus favour a short and efficient food web with increased fisheries potential.

The benefit of diatoms for crustaceans, however, is not universal. A range of diatom defences can function in naturally eutrophic systems with regular diatom blooms, despite the selective pressure in grazers to overcome them (Ianora and Miralto, 2010; Pancic et al., 2019). These mechanisms that hamper trophic transfer may prove more severe under artificial upwelling, where oligotrophic zooplankton conditioned to low diatom abundances dominate, at least initially (Hernandez-Leon, 1998; Mojica et al., 2015). We observed two changes under high Si upwelling that may impede grazing by crustaceans: the prominence of mineral shells that complicate mechanical handling and add ballast during digestion (Pancic et al., 2019) and the unusually high carbon to nutrient ratio that lead to nutritional imbalance (Anderson et al., 2005; Steinberg et al., 2017). Eventually, the benefit of Si upwelling for fisheries production may hinge on the presence of crustacean grazers that are highly adapted to silicified food of low nutritional value.

Conclusion

We identify Si:N nutrient stoichiometry as a strong driver of plankton bloom quality, and to a lesser extent quantity, during artificial upwelling (Figure 6). This Si-effect is likely to interact with major design aspects of an upwelling facility, such as the mode and duration of nutrient provisioning. Being constrained to a short time window, the effect on carbon assimilation may be taken advantage of by a stationary facility where a water mass receives only a single pulse of nutrients ('plume' type fertilization). The increase of phytoplankton size and mineral ballast by high Si proved instead more stable over time. These community properties may thus benefit a free-floating facility that maintains the eutrophic state long-term ('patch' type fertilisation). In any case, the chosen Si-strategy may not be capable to improve trophic transfer and carbon sequestration simultaneously. Maximizing CO_2 removal *via* mineral ballast and high carbon to nutrient ratios of organic matter implies a low food palatability that may, in turn, impair trophic transfer in the absence of highly adapted crustacean grazers.

The insights provided herein are limited to the growth-phase of the bloom. An entirely different response to Si could emerge under post-bloom dynamics, when upwelling is discontinued and plankton falls out en mass. We are clearly only beginning to understand the potential and risks of artificial upwelling as negative emission technology and ecosystem-based aquaculture.

Time is running out to evaluate such nature-based solutions for society's path out of the climate crisis and towards global food security.

Data availability statement

The raw data supporting the conclusions of this article will be made available by the authors, without undue reservation, *via* PANGAEA (https://www.pangaea.de/?q=campaign:%22KOSMOS_2019%22).

Author contributions

All authors designed the study and conducted the experiment. SG analyzed the data. SG wrote the manuscript with input from all authors. All authors contributed to the article and approved the submitted version.

Funding

This study was conducted within the projects Ocean Artificial Upwelling (Ocean artUp) funded by an Advanced Grant of the European Research Council and Road Testing Ocean Artificial Upwelling (Test-ArtUp) funded by the German Marine Research Alliance (DAM). Further support was provided through Transnational Access funds by the EU project AQUACOSM and by project TRIATLAS (AMD-817578-5) from the European Union's Horizon 2020. JA was also supported by a Helmholtz International Fellow Award, 2015 (Helmholtz Association, Germany).

Acknowledgments

We thank the Plataforma Oceánica de Canarias (PLOCAN) for providing facilities and logistical and technical support throughout the experiment. Further, we thank all the staff and students from the KOSMOS team of GEOMAR and the biological oceanography group of ULPGC who organised and carried out the experiment and Greta Wunderlich for her microscopical assessment of the phytoplankton community.

Conflict of interest

The authors declare that the research was conducted in the absence of any commercial or financial relationships that could be construed as a potential conflict of interest.

Publisher's note

Supplementary material

The Supplementary Material for this article can be found online at: https://www.frontiersin.org/articles/10.3389/fmars.2022.1015188/full#supplementary-material

References

Allen, J. T., Brown, L., Sanders, R., Moore, C. M., Mustard, A., Fielding, S., et al. (2005). Diatom carbon export enhanced by silicate upwelling in the northeast Atlantic. *Nature* 437, 728–732. doi: 10.1038/nature03948

Anderson, T. R., Hessen, D. O., Elser, J. J., and Urabe, J. (2005). Metabolic stoichiometry and the fate of excess carbon and nutrients in consumers. *Am. Nat.* 165, 1–15. doi: 10.1086/426598

Aristegui, J., Hernandez-Leon, S., Montero, M. F., and Gomez, M. (2001). The seasonal planktonic cycle in coastal waters of the canary islands. *Scientia Marina* 65, 51–58. doi: 10.3989/scimar.2001.65s151

Armengol, L., Calbet, A., Franchy, G., Rodriguez-Santos, A., and Hernandez-Leon, S. (2019). Planktonic food web structure and trophic transfer efficiency along a productivity gradient in the tropical and subtropical Atlantic ocean. *Sci. Rep.* 9, 19. doi: 10.1038/s41598-019-38507-9

Armstrong, R. A., Lee, C., Hedges, J. I., Honjo, S., and Wakeham, S. G. (2001). A new, mechanistic model for organic carbon fluxes in the ocean based on the quantitative association of POC with ballast minerals. *Deep-Sea Res. Part Ii-Topical Stud. Oceanogr.* 49, 219–236. doi: 10.1016/S0967-0645(01)00101-1

Bach, L. T., Hernandez-Hernandez, N., Taucher, J., Spisla, C., Sforna, C., Riebesell, U., et al. (2019). Effects of elevated CO2 on a natural diatom community in the subtropical NE Atlantic. *Front. Mar. Sci.* 6, 16. doi: 10.3389/fmars.2019.00075

Ban, S. H., Burns, C., Castel, J., Chaudron, Y., Christou, E., Escribano, R., et al. (1997). The paradox of diatom-copepod interactions. *Mar. Ecol. Prog. Ser.* 157, 287–293. doi: 10.3354/meps157287

Barlow, R. G., Cummings, D. G., and Gibb, S. W. (1997). Improved resolution of mono- and divinyl chlorophylls a and b and zeaxanthin and lutein in phytoplankton extracts using reverse phase c-8 HPLC. *Mar. Ecol. Prog. Ser.* 161, 303–307. doi: 10.3354/meps161303

Barton, E., Arıstegui, J., Tett, P., Cantón, M., Garcıa-Braun, J., Hernández-León, S., et al. (1998). The transition zone of the canary current upwelling region. *Prog. Oceanogr.* 41, 455–504. doi: 10.1016/S0079-6611(98)00023-8

Bates, D., Machler, M., Bolker, B. M., and Walker, S. C. (2015). Fitting linear mixed-effects models using lme4. *J. Stat. Software* 67, 1–48. doi: 10.18637/jss.v067.i01

Baumann, M., Taucher, J., Paul, A. J., Heinemann, M., Vanharanta, M., Bach, L. T., et al. (2021). Effect of intensity and mode of artificial upwelling on particle flux and carbon export. *Front. Mar. Sci.* 1579. doi: 10.3389/fmars.2021.742142

Bibby, T. S., and Moore, C. M. (2011). Silicate: nitrate ratios of upwelled waters control the phytoplankton community sustained by mesoscale eddies in sub-tropical north Atlantic and pacific. *Biogeosciences* 8, 657–666. doi: 10.5194/bg-8-657-2011

Boxhammer, T., Bach, L. T., Czerny, J., and Riebesell, U. (2016). Technical note: Sampling and processing of mesocosm sediment trap material for quantitative biogeochemical analysis. *Biogeosciences* 13, 2849–2858. doi: 10.5194/bg-13-2849-2016

Boyce, D. G., Lewis, M. R., and Worm, B. (2010). Global phytoplankton decline over the past century. *Nature* 466, 591–596. doi: 10.1038/nature09268

Boyd, P. W., Claustre, H., Levy, M., Siegel, D. A., and Weber, T. (2019). Multi-faceted particle pumps drive carbon sequestration in the ocean. *Nature* 568, 327–335. doi: 10.1038/s41586-019-1098-2

Chassot, E., Bonhommeau, S., Dulvy, N. K., Melin, F., Watson, R., Gascuel, D., et al. (2010). Global marine primary production constrains fisheries catches. *Ecol. Lett.* 13, 495–505. doi: 10.1111/j.1461-0248.2010.01443.x

Chavez, F. P., and Messie, M. (2009). A comparison of Eastern boundary upwelling ecosystems. *Prog. Oceanogr.* 83, 80–96. doi: 10.1016/j.pocean.2009.07.032

Core Team, R. (2021). *R: A language and environment for statistical computing* (Vienna, Austria: R Foundation for Statistical Computing).

Costello, C., Cao, L., Gelcich, S., Cisneros-Mata, M. A., Free, C. M., Froehlich, H. E., et al. (2020). The future of food from the sea. *Nature* 588, 95–100. doi: 10.1038/s41586-020-2616-y

Cury, P., Bakun, A., Crawford, R. J. M., Jarre, A., Quinones, R. A., Shannon, L. J., et al. (2000). Small pelagics in upwelling systems: patterns of interaction and structural changes in "wasp-waist" ecosystems. *Ices J. Mar. Sci.* 57, 603–618. doi: 10.1006/jmsc.2000.0712

Cushing, D. H. (1989). A difference in structure between ecosystems in strongly stratified waters and in those that are only weakly stratified. *J. Plankton Res.* 11, 1–13. doi: 10.1093/plankt/11.1.1

Decima, M., and Landry, M. R. (2020). Resilience of plankton trophic structure to an eddy-stimulated diatom bloom in the north pacific subtropical gyre. *Mar. Ecol. Prog. Ser.* 643, 33–48. doi: 10.3354/meps13333

Dickson, A. G., Afghan, J. D., and Anderson, G. C. (2003). Reference materials for oceanic CO2 analysis: a method for the certification of total alkalinity. *Mar. Chem.* 80, 185–197. doi: 10.1016/S0304-4203(02)00133-0

Dickson, A. G., Sabine, C. L., and Christian, J. R. (2007). *Guide to best practices for ocean CO2 measurements* (Sidney, BC, Canada: North Pacific Marine Science Organization).

Dubelaar, G. B. J., and Jonker, R. R. (2000). Flow cytometry as a tool for the study of phytoplankton. *Scientia Marina* 64, 135–156. doi: 10.3989/scimar.2000.64n2135

Dugdale, R. C., and Wilkerson, F. P. (1998). Silicate regulation of new production in the equatorial pacific upwelling. *Nature* 391, 270–273. doi: 10.1038/34630

Dulaquais, G., Boye, M., Rijkenberg, M. J. A., and Carton, X. (2014). Physical and remineralization processes govern the cobalt distribution in the deep western Atlantic ocean. *Biogeosciences* 11, 1561–1580. doi: 10.5194/bg-11-1561-2014

Dutkiewicz, S., Boyd, P. W., and Riebesell, U. (2021). Exploring biogeochemical and ecological redundancy in phytoplankton communities in the global ocean. *Global Change Biol.* 27, 1196–1213. doi: 10.1111/gcb.15493

Dutreuil, S., Bopp, L., and Tagliabue, A. (2009). Impact of enhanced vertical mixing on marine biogeochemistry: lessons for geo-engineering and natural variability. *Biogeosciences* 6, 901–912. doi: 10.5194/bg-6-901-2009

Eddy, T. D., Bernhardt, J. R., Blanchard, J. L., Cheung, W. W., Colléter, M., Du Pontavice, H., et al. (2020). Energy flow through marine ecosystems: Confronting transfer efficiency. *Trends Ecol. Evol* 36:76–86. doi: 10.1016/j.tree.2020.09.006

Edler, L., and Elbrächter, M. (2010). The utermöhl method for quantitative phytoplankton analysis. *Microscopic Mol. Methods quantitative phytoplankton Anal.* 110, 13–20.

Eppley, R. W., and Peterson, B. J. (1979). Particulate organic-matter flux and planktonic new production in the deep ocean. *Nature* 282, 677–680. doi: 10.1038/282677a0

Espinoza, P., and Bertrand, A. (2008). Revisiting Peruvian anchovy (Engraulis ringens) trophodynamics provides a new vision of the Humboldt current system. *Prog. Oceanogr.* 79, 215–227. doi: 10.1016/j.pocean.2008.10.022

Fuhrman, J., McJeon, H., Patel, P., Doney, S. C., Shobe, W. M., and Clarens, A. F. (2020). Food-energy-water implications of negative emissions technologies in a+1.5 degrees c future. *Nat. Clim. Change* 10, 920. doi: 10.1038/s41558-020-0876-z

Fu, W. W., Randerson, J. T., and Moore, J. K. (2016). Climate change impacts on net primary production (NPP) and export production (EP) regulated by increasing stratification and phytoplankton community structure in the CMIP5 models. *Biogeosciences* 13, 5151–5170. doi: 10.5194/bg-13-5151-2016

Gattuso, J.-P., Williamson, P., Duarte, C. M., and Magnan, A. K. (2021). The potential for ocean-based climate action: negative emissions technologies and beyond. *Front. Climate* 2, 37. doi: 10.3389/fclim.2020.575716

Geider, R. J., and La Roche, J. (2002). Redfield revisited: variability of c : N : P in marine microalgae and its biochemical basis. *Eur. J. Phycology* 37, 1–17. doi: 10.1017/S0967026201003456

Gilpin, L. C., Davidson, K., and Roberts, E. C. (2004). The influence of changes in nitrogen: silicon ratios on diatom growth dynamics. *J. Sea Res.* 51, 21–35. doi: 10.1016/j.seares.2003.05.005

Godfray, H. C. J., Beddington, J. R., Crute, I. R., Haddad, L., Lawrence, D., Muir, J. F., et al. (2010). Food security: The challenge of feeding 9 billion people. *Science* 327, 812–818. doi: 10.1126/science.1185383

Gohin, F. (2011). Annual cycles of chlorophyll-a, non-algal suspended particulate matter, and turbidity observed from space and *in-situ* in coastal waters. *Ocean Sci.* 7, 705–732. doi: 10.5194/os-7-705-2011

Granum, E., Kirkvold, S., and Myklestad, S. M. (2002). Cellular and extracellular production of carbohydrates and amino acids by the marine diatom skeletonema costatum: diel variations and effects of n depletion. *Mar. Ecol. Prog. Ser.* 242, 83–94. doi: 10.3354/meps242083

Griffiths, J. D., Barker, S., Hendry, K. R., Thornalley, D. J. R., van de Flierdt, T., Hall, I. R., et al. (2013). Evidence of silicic acid leakage to the tropical Atlantic *via* Antarctic intermediate water during marine isotope stage 4. *Paleoceanography* 28, 307–318. doi: 10.1002/palo.20030

Hansen, H. P., and Koroleff, F. (1999). *Determination of nutrients* (Weinheim, Germany: Wiley-VCH).

Harris, R. P., Irigoien, X., Head, R. N., Rey, C., Hygum, B. H., Hansen, B. W., et al. (2000). Feeding, growth, and reproduction in the genus calanus. *Ices J. Mar. Sci.* 57, 1708–1726. doi: 10.1006/jmsc.2000.0959

Hernandez-Leon, S. (1998). Annual cycle of epiplanktonic copepods in canary island waters. *Fisheries Oceanogr.* 7, 252–257. doi: 10.1046/j.1365-2419.1998.00071.x

Hessen, D. O., Agren, G. I., Anderson, T. R., Elser, J. J., and De Ruiter, P. C. (2004). Carbon, sequestration in ecosystems: The role of stoichiometry. *Ecology* 85, 1179–1192. doi: 10.1890/02-0251

Holmes, R. M., Aminot, A., Kerouel, R., Hooker, B. A., and Peterson, B. J. (1999). A simple and precise method for measuring ammonium in marine and freshwater ecosystems. *Can. J. Fisheries Aquat. Sci.* 56, 1801–1808. doi: 10.1139/f99-128

Ianora, A., and Miralto, A. (2010). Toxigenic effects of diatoms on grazers, phytoplankton and other microbes: a review. *Ecotoxicology* 19, 493–511. doi: 10.1007/s10646-009-0434-y

IPCC and Core Writing Team (2014). "Climate change 2014: Synthesis report," in *Contribution of working groups I, II and III to the fifth assessment report of the intergovernmental panel on climate change*. Eds. R. K. Pachauri and L. A. Meyer (Geneva, Switzerland: IPCC).

Jin, X., Gruber, N., Dunne, J. P., Sarmiento, J. L., and Armstrong, R. A. (2006). Diagnosing the contribution of phytoplankton functional groups to the production and export of particulate organic carbon, CaCO3, and opal from global nutrient and alkalinity distributions. *Global Biogeochem. Cycles* 20. doi: 10.1029/2005GB002532

Karl, D. M., and Letelier, R. M. (2008). Nitrogen fixation-enhanced carbon sequestration in low nitrate, low chlorophyll seascapes. *Mar. Ecol. Prog. Ser.* 364, 257–268. doi: 10.3354/meps07547

Kleppel, G. S. (1993). On the diets of calanoid copepods. *Mar. Ecol. Prog. Ser.* 99, 183–195. doi: 10.3354/meps099183

Kuznetsova, A., Brockhoff, P. B., and Christensen, R. H. B. (2017). lmerTest package: Tests in linear mixed effects models. *J. Stat. Software* 82, 1–26. doi: 10.18637/jss.v082.i13

Landry, M. R. (2002). Integrating classical and microbial food web concepts: evolving views from the open-ocean tropical pacific. *Hydrobiologia* 480, 29–39. doi: 10.1023/A:1021272731737

Llinás, O., Leon, A., Siedler, G., and Wefer, G. (1999). ESTOC data report 95/96. *Instituto Canario Cienc. Marinas Telde*.

Macreadie, P. I., Costa, M. D. P., Atwood, T. B., Friess, D. A., Kelleway, J. J., Kennedy, H., et al. (2021). Blue carbon as a natural climate solution. *Nat. Rev. Earth Environ* 2:826–839. doi: 10.1038/s43017-021-00224-1

Makareviciute-Fichtner, K., Matthiessen, B., Lotze, H. K., and Sommer, U. (2021). Phytoplankton nutritional quality is altered by shifting Si:N ratios and selective grazing. *J. Plankton Res.* 43, 325–337. doi: 10.1093/plankt/fbab034

Mari, X., Passow, U., Migon, C., Burd, A. B., and Legendre, L. (2017). Transparent exopolymer particles: Effects on carbon cycling in the ocean. *Prog. Oceanogr.* 151, 13–37. doi: 10.1016/j.pocean.2016.11.002

Martiny, A. C., Vrugt, J. A., Primeau, F. W., and Lomas, M. W. (2013). Regional variation in the particulate organic carbon to nitrogen ratio in the surface ocean. *Global Biogeochemical Cycles* 27, 723–731. doi: 10.1002/gbc.20061

Matear, R. J., and Hirst, A. C. (1999). Climate change feedback on the future oceanic CO2 uptake. *Tellus Ser. B-Chem. Phys. Meteorol.* 51, 722–733. doi: 10.3402/tellusb.v51i3.16472

Messie, M., Ledesma, J., Kolber, D. D., Michisaki, R. P., Foley, D. G., and Chavez, F. P. (2009). Potential new production estimates in four eastern boundary upwelling ecosystems. *Prog. Oceanogr.* 83, 151–158. doi: 10.1016/j.pocean.2009.07.018

Minx, J. C., Lamb, W. F., Callaghan, M. W., Fuss, S., Hilaire, J., Creutzig, F., et al. (2018). Negative emissions-part 1: Research landscape and synthesis. *Environ. Res. Lett.* 13:063001. doi: 10.1088/1748-9326/aabf9b

Mitchell, J. G., Seuront, L., Doubell, M. J., Losic, D., Voelcker, N. H., Seymour, J., et al. (2013). The role of diatom nanostructures in biasing diffusion to improve uptake in a patchy nutrient environment. *PloS One* 8, e59548. doi: 10.1371/journal.pone.0059548

Mojica, K. D. A., van de Poll, W. H., Kehoe, M., Huisman, J., Timmermans, K. R., Buma, A. G. J., et al. (2015). Phytoplankton community structure in relation to vertical stratification along a north-south gradient in the northeast Atlantic ocean. *Limnol. Oceanogr.* 60, 1498–1521. doi: 10.1002/lno.10113

Moore, C. M., Mills, M. M., Arrigo, K. R., Berman-Frank, I., Bopp, L., Boyd, P. W., et al. (2013). Processes and patterns of oceanic nutrient limitation. *Nat. Geosci.* 6, 701–710. doi: 10.1038/ngeo1765

Neuer, S., Cianca, A., Helmke, P., Freudenthal, T., Davenport, R., Meggers, H., et al. (2007). Biogeochemistry and hydrography in the eastern subtropical north Atlantic gyre. results from the European time-series station ESTOC. *Prog. Oceanogr.* 72, 1–29. doi: 10.1016/j.pocean.2006.08.001

Olenina, I. (2006). Biovolumes and size-classes of phytoplankton in the Baltic Sea. *HELCOM Baltic Sea Environ. Proc. No.106*. 144.

Ortiz, J., Arístegui, J., Taucher, J., and Riebesell, U. (2022). Artificial upwelling in singular and recurring mode: Consequences for net community production and metabolic balance. *Front. Mar. Sci.* 8. doi: 10.3389/fmars.2021.743105

Pancic, M., Torres, R. R., Almeda, R., and Kiorboe, T. (2019). Silicified cell walls as a defensive trait in diatoms. *Proc. R. Soc. B-Biol. Sci.* 286, 9. doi: 10.1098/rspb.2019.0184

Pan, Y. W., Wei, F., Zhang, D. H., Chen, J. W., Huang, H. C., Liu, S. X., et al. (2016). Research progress in artificial upwelling and its potential environmental effects. *Sci. China-Earth Sci.* 59, 236–248. doi: 10.1007/s11430-015-5195-2

Paul, A. J., Bach, L. T., Schulz, K. G., Boxhammer, T., Czerny, J., Achterberg, E. P., et al. (2015). Effect of elevated CO2 on organic matter pools and fluxes in a summer Baltic Sea plankton community. *Biogeosciences* 12, 6181–6203. doi: 10.5194/bg-12-6181-2015

Pauly, D., and Christensen, V. (1995). Primary production required to sustain global fisheries. *Nature* 374, 255–257. doi: 10.1038/374255a0

Pielou, E. C. (1966). The measurement of diversity in different types of biological collections. *J. Theor. Biol.* 13, 131–144. doi: 10.1016/0022-5193(66)90013-0

Pitcher, G. C., Walker, D. R., Mitchellinnes, B. A., and Moloney, C. L. (1991). Short-term variability during an anchor station study in the southern benguela upwelling system – phytoplankton dynamics. *Prog. Oceanogr.* 28, 39–64. doi: 10.1016/0079-6611(91)90020-M

Polovina, J. J., Howell, E. A., and Abecassis, M. (2008). Ocean's least productive waters are expanding. *Geophysical Res. Lett.* 35, 5. doi: 10.1029/2007GL031745

Popescu, I., and Ortega Gras, J. J. (2015). Fisheries in the canary islands. *European Parliament, Directorate-General for Internal Policies of the Union*. doi: 10.2861/18051

Quinn, G. P., and Keough, M. J. (2002). *Experimental design and data analysis for biologists* (New York, USA: Cambridge University Press).

Ragueneau, O., Treguer, P., Leynaert, A., Anderson, R. F., Brzezinski, M. A., DeMaster, D. J., et al. (2000). A review of the Si cycle in the modem ocean: recent progress and missing gaps in the application of biogenic opal as a paleoproductivity proxy. *Global Planetary Change* 26, 317–365. doi: 10.1016/S0921-8181(00)00052-7

Redfield, A. C. (1958). The biological control of chemical factors in the environment. *Am. Sci.* 46, 205–221.

Riebesell, U., Czerny, J., von Brockel, K., Boxhammer, T., Budenbender, J., Deckelnick, M., et al. (2013). Technical note: A mobile sea-going mesocosm system - new opportunities for ocean change research. *Biogeosciences* 10, 1835–1847. doi: 10.5194/bg-10-1835-2013

Riquelme-Bugueno, R., Pantoja-Gutierrez, S., Jorquera, E., Anabalon, V., Srain, B., and Schneider, W. (2020). Fatty acid composition in the endemic Humboldt current krill, euphausia mucronata (Crustacea, euphausiacea) in relation to the phytoplankton community and oceanographic variability off dichato coast in central Chile. *Prog. Oceanogr.* 188, 11. doi: 10.1016/j.pocean.2020.102425

Romann, J., Valmalette, J. C., Chauton, M. S., Tranell, G., Einarsrud, M. A., and Vadstein, O. (2015). Wavelength and orientation dependent capture of light by diatom frustule nanostructures. *Sci. Rep.* 5, 6. doi: 10.1038/srep17403

Rosenfeld, J. S. (2002). Functional redundancy in ecology and conservation. *Oikos* 98, 156–162. doi: 10.1034/j.1600-0706.2002.980116.x

RStudio Team (2021). *RStudio: Integrated development environment for r* (Boston, MA: RStudio, PBC).

Ryther, J. H. (1969). Photosynthesis and fish production in the sea. *Science* 166, 72–76. doi: 10.1126/science.166.3901.72

Sarmiento, J. L., Gruber, N., Brzezinski, M. A., and Dunne, J. P. (2004). High-latitude controls of thermocline nutrients and low latitude biological productivity. *Nature* 427, 56–60. doi: 10.1038/nature02127

Sarthou, G., Timmermans, K. R., Blain, S., and Treguer, P. (2005). Growth physiology and fate of diatoms in the ocean: A review. *J. Sea Res.* 53, 25–42. doi: 10.1016/j.seares.2004.01.007

Sathyendranath, S., Stuart, V., Nair, A., Oka, K., Nakane, T., Bouman, H., et al. (2009). Carbon-to-chlorophyll ratio and growth rate of phytoplankton in the sea. *Mar. Ecol. Prog. Ser.* 383, 73–84. doi: 10.3354/meps07998

Schulz, K. G., and Riebesell, U. (2013). Diurnal changes in seawater carbonate chemistry speciation at increasing atmospheric carbon dioxide. *Mar. Biol.* 160, 1889–1899. doi: 10.1007/s00227-012-1965-y

Sharp, J. H. (1974). Improved analysis for "particulate" organic carbon and nitrogen from seawater. *Limnol. Oceanogr.* 19, 984–989. doi: 10.4319/lo.1974.19.6.0984

Singmann, H., and Kellen, D. (2019). An introduction to mixed models for experimental psychology. *New Methods Cogn. Psychol.* 28, 4–31. doi: 10.4324/9780429318405-2

Smetacek, V. (1999). Diatoms and the ocean carbon cycle. *Protist* 150, 25–32. doi: 10.1016/S1434-4610(99)70006-4

Smith, M. D., Knapp, A. K., and Collins, S. L. (2009). A framework for assessing ecosystem dynamics in response to chronic resource alterations induced by global change. *Ecology* 90, 3279–3289. doi: 10.1890/08-1815.1

Sommer, U., Stibor, H., Katechakis, A., Sommer, F., and Hansen, T. (2002). Pelagic food web configurations at different levels of nutrient richness and their implications for the ratio fish production: primary production. *Hydrobiologia* 484, 11–20. doi: 10.1023/A:1021340601986

Steinacher, M., Joos, F., Frolicher, T. L., Bopp, L., Cadule, P., Cocco, V., et al. (2010). Projected 21st century decrease in marine productivity: a multi-model analysis. *Biogeosciences* 7, 979–1005. doi: 10.5194/bg-7-979-2010

Steinberg, D. K., Landry, M. R., and Annual, R. (2017). Zooplankton and the ocean carbon cycle. *Annu. Rev. Mar. Sci.* 9, 413–444. doi: 10.1146/annurev-marine-010814-015924

Stuart, V. (1989). Observations on the feeding of euphausia lucens on natural phytoplankton suspensions in the southern benguela upwelling region. *Continent. Shelf Res.* 9, 1017–1028. doi: 10.1016/0278-4343(89)90005-8

Tacon, A. G. J., and Metian, M. (2015). Feed matters: Satisfying the feed demand of aquaculture. *Rev. Fisheries Sci. Aquaculture* 23, 1–10. doi: 10.1080/23308249.2014.987209

Takahashi, T., Feely, R. A., Weiss, R. F., Wanninkhof, R. H., Chipman, D. W., Sutherland, S. C., et al. (1997). Global air-sea flux of CO2: An estimate based on measurements of sea-air pCO2 difference. *Proc. Natl. Acad. Sci. U. S. A.* 94, 8292–8299. doi: 10.1073/pnas.94.16.8292

Talmy, D., Blackford, J., Hardman-Mountford, N. J., Polimene, L., Follows, M. J., and Geider, R. J. (2014). Flexible c : N ratio enhances metabolism of large phytoplankton when resource supply is intermittent. *Biogeosciences* 11, 4881–4895. doi: 10.5194/bg-11-4881-2014

Taucher, J., Bach, L. T., Boxhammer, T., Nauendorf, A., Achterberg, E. P. , Algueró-Muñiz, M., et al. (2017). Influence of ocean acidification and deep water upwelling on oligotrophic plankton communities in the subtropical north Atlantic: insights from an *in situ* mesocosm study. *Front. Mar. Sci.* 4, 85. doi: 10.3389/fmars.2017.00085

Thornton, D. C. O. (2002). Diatom aggregation in the sea: Mechanisms and ecological implications. *Eur. J. Phycology* 37, 149–161. doi: 10.1017/S0967026202003657

Veldhuis, M. J. W., and Kraay, G. W. (2000). Application of flow cytometry in marine phytoplankton research: current applications and future perspectives. *Scientia Marina* 64, 121–134. doi: 10.3989/scimar.2000.64n2121

Vihtakari, M. (2021). *ggOceanMaps: Plot data on oceanographic maps using 'ggplot2'* (R package). Available at: https://CRAN.R-project.org/package=ggOceanMaps.

Yool, A., Shepherd, J. G., Bryden, H. L., and Oschlies, A. (2009). Low efficiency of nutrient translocation for enhancing oceanic uptake of carbon dioxide. *J. Geophysical Research-Oceans* 114, C08009. doi: 10.1029/2008JC004792